SCIENCE CHINA
Physics, Mechanics & Astronomy

• Invited Review•

October 2015 Vol. 58 No. 10: 107401
doi: 10.1007/s11433-015-5701-8

Research trends in electron-doped cuprate superconductors

YUAN Jie, HE Ge, YANG Hua, SHI YuJun, ZHU BeiYi & JIN Kui*

Beijing National Laboratory for Condensed Matter Physics, Institute of Physics, Chinese Academy of Sciences, Beijing 100190, China

Received April 16, 2015; accepted May 22, 2015

In this review, we look back on some intriguing and puzzling issues in electron-doped cuprate superconductors, such as electron-hole asymmetry, two types of carriers, quantum critical points, order-parameter symmetry, etc. The necessity of study on this family is invoked in comparison with the hole-doped counterparts from several aspects. The related progress, especially in last few years, has been outlined point to point, as well as other hot topics like the discovery of ambipolar superconductors, the applications in superconducting electronics, and the emergency of superconductivity in parent compounds. In perspective, the utilization of blooming advanced techniques, electric double layer transistor and combinatorial film deposition, will bring some new insights into the mechanism such as electron-doped cuprate superconductors.

electron-doped, electronic structure, quantum critical phenomena

PACS number(s): 74.72.Ek, 74.25.Jb, 74.40.Kb

Citation: Yuan J, He G, Yang H, et al. Research trends in electron-doped cuprate superconductors. Sci China-Phys Mech Astron, 2015, 58: 107401, doi: 10.1007/s11433-015-5701-8

1 Introduction

The superconductivity in perovskite Ba-La-Cu-O was first discovered in 1986 by Karl Müller and Johannes Bednorz [1], for which they were awarded the Nobel Prize in Physics in 1987. This broke the fastest world record for the award grant and opened a prelude to the study of high temperature superconductor (HTS). So far, $HgBa_2Ca_2Cu_3O_{8+\delta}$ holds the record of the highest T_c, i.e. 134 K at ambient pressure [2] and 164 K under high pressure [3].

The high-temperature cuprate superconductors are based on a certain class of ceramic materials. All share the common feature: layered perovskite-like crystal structures consisting of square planar copper-oxygen layers separated by charge reservoir layers. These reservoir layers serve to donate charge carriers to the CuO_2 planes. According to the sign of carriers introduced into CuO_2 layers, the cuprate superconductors are categorized into hole- and electron-doped types. Although the overwhelming majority of high-T_c cuprate superconductors are hole-doped, there exists a nontrivial family of electron-doped compounds [4]. Hitherto, there are only two classes of electron-doped cuprates. One is the 214-type superconductor, belonging to point group D_{4h}^{17} and space group $I4/mmm$. The other is the so-called infinite layer superconductor of point group D_{4h}^{1} and space group $P4/mmm$.

Most electron-doped materials possess the 214 structure, i.e. the chemical formula as $Ln_{2-x}M_xCuO_4$, where Ln = Pr, Nd, Sm, or Eu and M = Ce or Th [5–8]. Compared to the hole-doped $La_{2-x}M_xCuO_4$ (M = Ca, Ba, Sr) superconductors of T phase, the electron-doped counterparts are of T' phase as shown in Figure 1. Although both are 214-type superconductors, there is significant difference between them. That is, the copper atoms and oxygen atoms form a planar structure in T' phase but an octahedron in T phase. Another distinction is that the electron-doped cuprates always hold the tetragonal structure as varying x, whereas the hole-doped one, e.g. $La_{2-x}Sr_xCuO_4$(LSCO) experiences an evolu-

*Corresponding author (email: kuijin@iphy.ac.cn)

tion from orthorhombic- to tetragonal-structure with increasing x. Though the first electron-doped superconductor $Nd_{2-x}Ce_xCuO_4$ (NCCO) was reported in 1989, soon after the discovery of $La_{2-x}Ba_xCuO_4$, the comprehension on electron-doped compounds is far behind their counterparts [9]. The major obstruction is ascribed to the quality of the samples. In preparation, factors like temperature, atmosphere/vacuum, (local) strain, annealing and etc. should be fully considered to achieve the best quality. Despite this, it is still essential to investigate this kind of materials, then to fully understand the mechanism of high-T_c superconductivity because of the limitation in the hole-doped family. Here, based on the comparison between the electron- and hole-doped cuprate superconductors, we elucidate some key topics in this family, and give a review to show the recent progress on these topics.

With the improvement of the sample quality, more and more precise and detailed experimental results about the electron-doped superconductors have been revealed. Thus, a comparison between the electron-doped cuprates and the hole-doped ones can be carried out. The most important goal in the study of high-T_c superconductors is to explain the mechanism of electron pairing and the symmetry of the ordering parameter, inspiring the exploration of materials with higher T_c. The experimental results on cuprates, e.g. Josephson effects [10], Andreev reflection [11], Little-Parks flux quantization [12,13], particle-hole mixing [14], etc., have proved the existence of Cooper pairs in superconducting phase. The spin singlet state of electron pairing has been determined by NMR as well [15]. In the hole-doped cuprates, the gap symmetry of $d_{x^2-y^2}$ has been confirmed by the penetration depth [16], angular resolved photoemission energy spectrum (ARPES) [17], phase sensitive [18], specific heat [19], thermal conductivity [20] measurements, and so on. Though there is a preliminary conclusion on the order parameter symmetry of high-T_c superconductors, no agreement on the pairing mechanism has been achieved. As for the unconventional superconductors, the superconducting state always competes with other adjacent ordering state. More and more experiments show that the breakdown of spin/charge/orbital ordering will benefit the emergence of superconductivity [21,22]. Therefore, in order to map out the evolution of electronic state, methods like chemical doping, pressure, magnetic field, dimension modulation, etc. are used to tune materials from the superconducting ground state(s) to other ground states, vice versa. Displayed in Figure 2, the main distinctions between electron- and hole-doped cuprates from the view of the electronic phase diagram are listed as follows.

(1) The antiferromagnetic (AF) Neel temperature (T_N) for the electron-doped cuprates decreases more slowly. Thus, the AF horizon is wider and seems to truncate the superconducting region.

(2) In the under-doped region of hole-doped side, there is a characteristic temperature boundary of pseudo-gap with its origin still in hot debate [23], while in the electron-doped side, it's known that short-range antiferromagnetism or fluctuations dominates the corresponding area. Since the origin is distinct from the definition of pseudo-gap, the so-called pseudo-gap boundary is not present there.

(3) In hole-doped side, the classic picture usually displayed a quantum critical point (QCP) in the superconducting dome, where the extrapolated boundaries of pseudo-gap and Fermi liquid regimes merge at 0 K [24]. Above the QCP, there is a finite temperature region, where the transport behavior in the normal-state is dominated by the quantum criticality, e.g. the resistivity is linear in temperature. This region is called "strange metal" area. However, some recent work showed that the Fermi liquid boundary actually is closer to high doping level, not intersecting the boundary of pseudo-gap. At present, the ending point of the Fermi liquid region is uncertain [25]. While for electron-doped cuprates the boundary of Fermi liquid is located at the end of the superconducting dome, that is, the Fermi liquid behavior recovers at the doping level once the super-

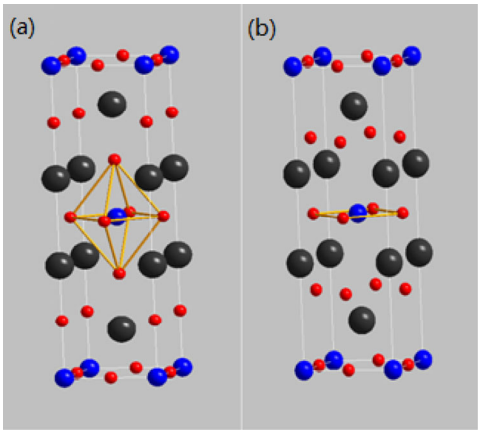

Figure 1 (Color online) Comparison of the T' and T structures. (a) Generic T structure with the atoms La as large black spheres, Cu as intermediate size blue spheres, and O as small red spheres. (b) T' structure shown with atoms Ln in black, O and Cu the same as in (a).

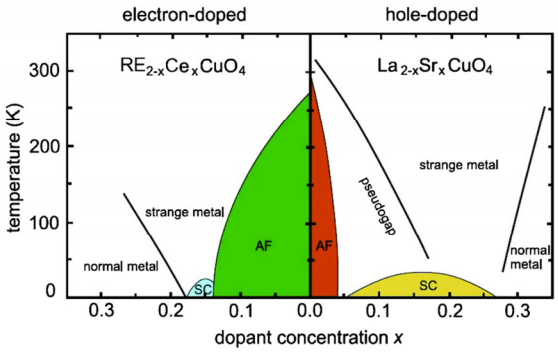

Figure 2 (Color online) Phase diagram of electron- and hole-doped cuprates [22].

conductivity disappears in zero field [26,27].

It is widely believed that unveiling the normal-state properties of the high-T_c cuprates is essential to the understanding of superconducting mechanism. But, some obstructions prevent the investigation on normal-state electronic states of hole-doped cuprates at low temperature. That is mainly because (1) it is difficult to suppress completely the superconductivity at low temperature, even if a pulsed magnetic field up to 60 Tesla is employed, (2) large magnetic field may result in the change of ground state (10 T ~ 1 meV). Whilst the ratio of signal to noise under pulsed field is not so good as that in static field, the information on evolution of the ground state becomes ambiguous as varying the magnetic field, (3) among the hole-doped cuprates, the *T*-linear dependent resistivity region is adjacent to the pseudo-gap area. The controversy on origin of pseudo-gap will add complexity on the investigation of microscopic mechanism in *T*-linear resistivity. In contrast, the upper critical field of electron-doped cuprate superconductors is much smaller (~10 T), subject to the range of static magnetic field. The normal-state electronic information can be thus obtained down to millKelvin temperature in a static magnetic field. Accordingly, more and more attention has been paid to the electron-doped cuprates.

There are quite a few frontiers in the research of electron-doped cuprates, such as electron-hole asymmetry, two types of charge carriers, order-parameter symmetry, quantum critical points, and so on. Besides, some new experimental phenomena have brought new inspirations into this field. It is impossible to review all of the topics in a short review paper. Here, we choose five hot topics and mainly focus on work in past few years. A comprehensive review on the electron-doped cuprates could be found in the ref. [9].

We start with a brief discussion on electron-hole asymmetry, e.g. the evolution of spin/charge ordered states upon electron- or hole-carrier doping. The second is about two types of charge carriers, which has been always an important issue since the discovery of electron-doped cuprates. The third is about QCP, where a continuous phase transition occurs at absolute zero temperature. The fourth is about the order-parameter symmetry. The fifth is a perspective on the superconductivity in parent compounds, challenging the conventional phase diagram.

2 Electron-hole asymmetry

In the phase diagram of cuprates, the most prominent feature is the presence of pseudo-gap in hole doping, which does not exist in the electron-doped side. This is an apparent electron-hole asymmetry in cuprates. The origin of such asymmetry is attributed to the persistency of the effective AF interaction against carrier doping. It has been argued that the next nearest t' term, in t-t'-J or t-t'-U model, is crucial to the strength of the AF state, i.e. the stability of the Neel configuration with up and down spins on different sublattices. The positive t', usually in electron-doped cuprates, will stabilize the eigenstate with a strong AF correlation as shown in Figure 3 [28].

Moritz et al. [29] investigated the particle-hole asymmetry in hole-doped LSCO and electron-doped NCCO via electronic Raman scattering. They found the asymmetry was associated with the on-site Coulomb repulsive correlated energy, i.e. Hubbard parameter *U*. Ishii et al. [30] tracked the doping dependence of both spin and charge excitations in NCCO and $Pr_{1.40-x}La_{0.60}Ce_xCuO_4$ (PLCCO) with resonant inelastic X-ray scattering (RIXS) and inelastic neutron scattering (INS). They revealed an electron-hole asymmetry in magnetic excitations, that is, the electron dynamics of the electron-doped cuprates had higher itinerant character in the sub-eV energy scale than that of hole-doping case in the overdoped region. This asymmetry was also found in the iron-based superconductors, where the features of pseudo-gap (PG) are much stronger in hole-doped than in electron-doped compounds, akin to the cuprates [31]. In addition, a possible electron-hole asymmetry is found to exist in the colossal magnetoresistive manganite phase diagram [32]. In this research, ultra-thin films of the electron-doped manganite $La_{0.8}Ce_{0.2}MnO_3$ were grown on (00*l*) oriented $SrTiO_3$ substrates by a pulsed laser interval deposition method. Hence, it seems that the study of asymmetry between electron- and hole-doped materials will deepen the understanding in nature of the cuprates, as well as other mimicking systems without loss of generality.

The existence of a PG in hole-doped high-T_c cuprate superconductors is a generally acknowledged fact. The debate is focused on the origin of the PG [33]. There are two types of PG: One is large-energy PG, which is comparable to the energy scale of the antiferromagnetic interaction [34]; the other is small-energy PG with a energy scale comparable to the superconducting gap [35]. On contrary to the hole-doped cuprates, the short-range AF order or fluctuations is

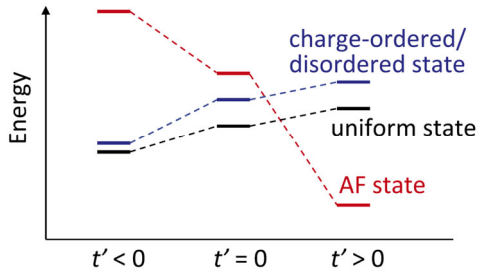

Figure 3 (Color online) Schematic energy diagram of the ground state and low-energy excited states for the t-t'-J model in underdoped region. $t' < 0$ and $t' > 0$ correspond to hole and electron dopings, respectively. When $t' > 0$, AF state is the most stable one in terms of its lowest energy level among all the possible states [28]. That may explain why the AF region of electron-doped is much broader than the counterpart of hole-doped in the phase diagram (Figure 2).

responsible for the corresponding "PG" area in electron-doped ones as mentioned above. However, the termination point of AF order is still in argument. For instance, the transport measurements on PCCO have shown a roughly consistent critical doping of ~ 0.16 [36,37], yet the INR results support a long range AF order to x ~ 0.13 [38]. In LCCO, there is a similar controversy between the transport and low-energy spin-polarized muons (LE-μSR) measurements as shown in Figure 4. This puzzle may be resulted from different response times of various detecting methods [33] or due to the interaction between the AF order and the superconductivity as proposed by Sachdev [39]. The latter means that there is an overlapped area of superconductivity and AF order, pointing to an asymmetry between electron- and hole-dopings.

Besides, a normal state gap (NSG) is suggested in electron-doped cuprates from point contact tunneling spectra [40–43]. Here, a depletion of the density of states near the Fermi level at a characteristic temperature T^* is a typical feature of the NSG (see Figure 5). The NSG (~ 5 meV)

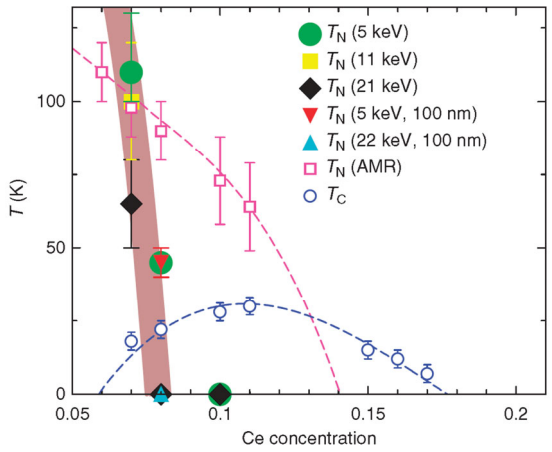

Figure 4 (Color online) Phase diagram of LCCO obtained from transport and LE-μSR. The open squares are Neel temperature from angular dependent in-plane magnetoresistivity measurement. Other symbols (T_N) are from the LE-μSR experiments [33].

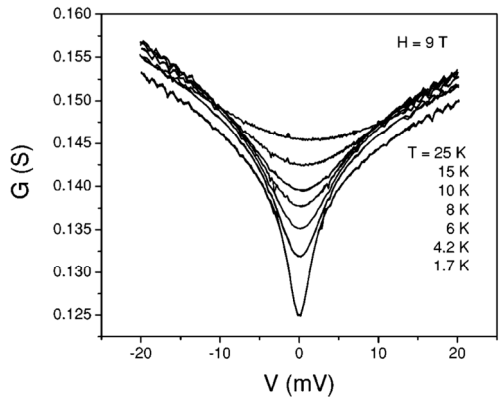

Figure 5 *G-V* curves of typical NSG feature. The *G-V* curves for the break junction between silver and PCCO (x =0.15) in different temperature at 9 T [40].

reported in electron-doped cuprates is different from the small PG found in hole-doped cuprates , e.g. ~ 62 meV in LSCO by optical conductivity measurements [44]. The NSG can be observed for $H > H_{c2}$ as well as for $T > T_c$ [40]. So far, the origin of the NSG is still unclear.

In last few years, charge/spin density waves, nematic order, etc., have been in hot debate for hole-doped cuprates [45–49]. In electron-doped cuprates, Neto et al. [50] found a charge order accompanied with the onset of spin-density-wave (or AF order). This work established a connection between the AF order by electric transport measurements and the so called "PG" defined by Onose et al. [51], who found a gap of ~ 0.3 eV in NCCO (x =0.15) by optical conductivity and Raman spectra measurements, attributed to a charge ordering instability promoted by a small amount of apical oxygen.

Very recently, a relation between the superconducting gap and the magnetic field, i.e. $\Delta \sim -B^2$, has been found in electron-doped NCCO and PLCCO as seen in Figure 6. The existence of such intriguing relationship implies a broken rotation symmetry of electronic states, e.g., an orbital-related state has been suggested to account for such relationship observed in $LiTi_2O_4$ superconductor [52]. While, there hasn't been any evidence for an orbital order or nematicity in electron-doped cuprates. It is also not easy to verify such relation in hole doped cuprates for their very high upper critical field. This mystery urges further investigations. Nevertheless, the observed $\Delta \sim -B^2$ by point contact measurements at least opens a window to probe the information on broken symmetry of electronic states.

3 Two types of carriers

In the under-doped region of hole-doped side, negative Hall coefficients had been observed in the quantum oscillation experiments [53,54]. The origin of the electron carriers and

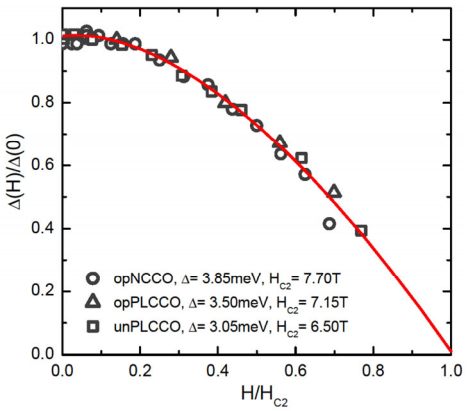

Figure 6 (Color online) Magnetic field dependence of gaps in optimal-doped of NCCO, PLCCO and under-doped PLCCO. The red line are the fitting data which are calculated by the formula $\Delta(H)/\Delta(0) = 1-(H/H_{C2})^2$ [52].

the location of corresponding Fermi surface in momentum space are still controversial. In latest view, this reconstruction of Fermi surface is thought to be caused by charge order (incommensurate charge-density-wave) [55]. However, the contribution from the vortices was also proposed [56].

As early as the discovery of electron-doped cuprates, anomalous behavior had been found in Hall resistivity, thermal power coefficient, Nernst effect measurements of $Nd_{1.85}Ce_{0.15}CuO_{4\pm\delta}$, which couldn't be well explained with single-band model [57]. Later, the coexistence of electron pocket near (π, 0) and the hole pocket near (π/2, π/2) has been confirmed by angular resolved photoemission energy spectra (ARPES) [58]. The low-temperature Hall effect of $La_{2-x}Ce_xCuO_4$ (LCCO) films was systematically studied over a much wider doping level from x = 0.06 to 0.17. It was found that with increasing x, the charge carriers gradually change from electron-like to hole-like as shown in Figure 7 [59]. Near the optimal doping level (x = 0.11), there are two types of charge carriers competing with each other [60]. Additionally, an anomalous sign reversal of Hall effect in mixed state may be ascribed to a flux-flow regime for two types of carriers with opposite charges [61,62].

Briefly, two theoretical models have been proposed. The first is considering the Fermi surface reconstruction by AF ordering. That is, two unit cells in real space form a magnetic unit cell, causing a reduction of the Brillouin zone and thus turning on the reconstruction of the Fermi surface due to instability at the hotspots. Therefore, a large hole Fermi surface evolves into small electron- and hole-pockets [63]. In an alternative view, electrons and holes come from the upper Hubbard band and the Zhang-Rice singlet band, respectively. In parent compounds (x=0), the hybridized Cu-O band is beneath the upper Hubbard band, i.e., there is a charge transfer gap of 1–2 eV between them [17]. With increasing the Ce doping level, electrons enter the upHubbard band, meanwhile attracting the hole band. Around the optimal doping, the electron- and hole- bands both cross the Fermi level [64].

In addition to the cation doping, the tuning of oxygen leads to a similar evolution of Fermi surface in electron-doped cuprates. Jiang et al. [65] changed the annealing condition for optimally doped NCCO, and observed a negative Hall coefficient gradually turning to positive with decreasing oxygen in the samples. Recently, the ARPES experiment on PLCCO verified that the hole pocket gradually appears in the deoxygenation process [66]. While in $YBa_2Cu_3O_{7-\delta}$ (YBCO), the reduction of oxygen will decrease the hole concentration, indicating distinct impacts of deoxygenation on electron- and hole-doped cuprates. This inspires more attention to the annealing process in understanding the nature of electron-doped cuprates.

It is well known that hole-doped LSCO favors T phase, while electron doped PCCO prefers T' phase. Curiously, the electron doping has been recently achieved in the T phase of PCCO by high-pressure method [67]. Not merely, by substitution of La for Ba, electrons can be doped into the YBCO system [68–70] (Figure 8). Thus, it is interesting to know what exactly happens, given two types of carriers doped into the same structure. This invokes the search of new ambipolar superconductors in future.

4 Quantum critical points

The study of quantum critical points (QCPs), derived from competing ground states at zero temperature, has been occupying a decisive position in unveiling the nature of unconventional superconductors [71]. In order to verify the quantum criticality of a critical point, a routine method is to drive the continuous phase transitions by non-thermal parameters, such as chemical doping, pressure, magnetic field

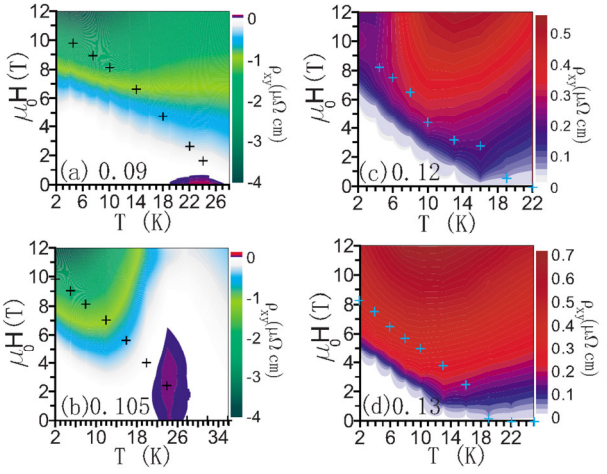

Figure 7 (Color online) Contour maps of $\rho_{xy}(H, T)$ for (a) x=0.09, (b) 0.105, (c) 0.12, and (d) 0.13. The sign and magnitude of $\rho_{xy}(H, T)$ could be distinguished by color bars [59].

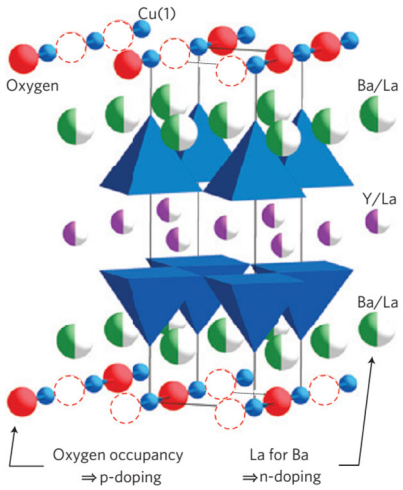

Figure 8 (Color online) Crystal structure of La-doped YBCO and the sites for chemical doping [70].

[72]. Very recently, electric double layer transistor has been successfully used to tune the cuprate superconductors like YBCO [73], LSCO [74], thin films.

A well-known anomaly associated with the quantum criticality is the linear temperature dependence of resistivity as $T \rightarrow 0$ at certain doping [75,76], usually associated to a QCP driven by antiferromagnetism in ideal two dimensional system [77] or in a slightly disordered three dimensional system [78]. While, recent study on hole-doped LSCO has revealed that the normal state resistivity contains a linear temperature dependent term over a wide regime in overdoped side once the superconductivity is suppressed in a pulsed high magnetic field. Moreover, the coefficient of the T-linear component, A_1, scales monotonically with the superconducting transition temperature [25]. This relation between A_1 and T_c has also been found in Nd-LSCO, $Ba(Fe_{1-x}Co_x)_2As_2$, YBCO, and Bechgaard Salt [79–81]. However, it should be pointed out that few cuprate systems can reach the boundary of the superconducting dome from the overdoped side. The Fermi liquid region, where $\rho = \rho_0 + A_2T^2$, is not accessible due to the restriction of solid solubility. The electron-doped cuprate LCCO is the rare one that can cover both the superconducting dome and the Fermi liquid region, yet only stabilized in form of thin film [82].

In this system, the relevance of QCPs and superconductivity has been studied by Jin et al. [26,27,83]. The *ab*-plane resistivity without external magnetic field can be fitted with the formula $\rho = \rho_0 + A_nT^n$. The values of n vary against the nominal Ce^{4+} doping at finite temperature as shown in Figure 9. n =1 and n = 2 represent pure linear resistivity and the Fermi liquid regions, respectively. It is interesting that the linear resistivity region, right above the superconducting dome, vanishes at the same point where the superconductivity disappears as well as the Fermi-liquid behavior turns out.

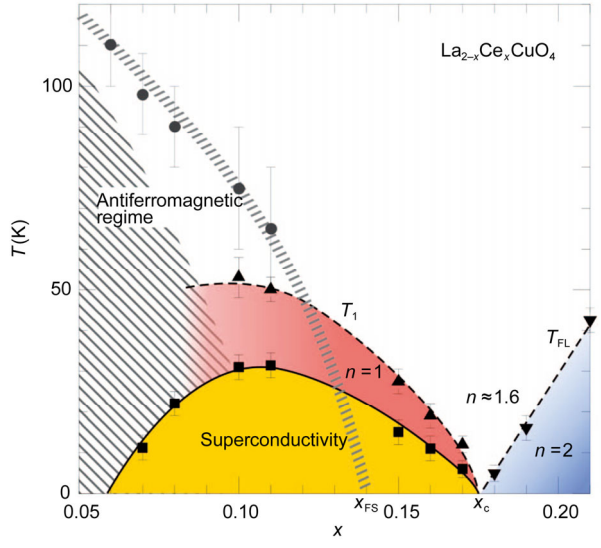

Figure 9 (Color online) Temperature-doping (T-x) phase diagram of $La_{2-x}Ce_xCuO_4$ [26].

The revealed critical doping, x_c = 0.175 at T = 0, undoubtedly points to an intimate relationship between the linear-temperature resistivity behavior and the superconductivity. As mentioned above, the pure T-linear resistivity (n = 1) as $T \rightarrow 0$ should be an indication of a QCP associated with the antiferromagnetism (spin-density-wave). While, this new phase diagram firstly presents a T-linear resistivity regime down to the lowest measuring temperature (20 mK). This result suggests an "extended quantum phase".

Note that the AF spin fluctuation is found to extend over the entire superconducting dome in PLCCO, as probed by inelastic neutron scattering experiments [84]. Sedeki et al. studied the normal-state properties of quasi-1D superconductors with the doping near a spin-density-wave instability with the renormalization group method. An extended quantum critical region is also found to be associated with evolution of T-linear resistivity in the phase diagram [85]. Nevertheless, none of theoretical models can explain the micro mechanism of this T-linear resistivity behavior.

In the phase diagram, there is another QCP hidden in the superconducting dome, i.e., at x_{FS} = 0.14, where the change of the sign of the low-temperature Hall coefficient [59], the disappearance of in-plane anisotropic magnetoresistance [83], and the metal to insulator transition [86] have been observed. The x_{FS} is linked to the reconstruction of Fermi surface, akin to the proved QCP at Ce = 0.16 in PCCO system [36,37].

The critical doping x_c was also confirmed to be a QCP from several aspects [27]. First, a universal power law, n = 1.6, governs the region divergent from the point x_c. Second, it should be proved that at this point, n = 1.6 can persist to zero temperature limit. It is impossible to obtain a chemical doping right at the QCP for the influence of oxygen and some other uncontrollable issues during the growth. While, it is found that applying a magnetic field can gradually shift this point to lower Ce level. Thus, the doping x = 0.17 at 4 T turns out to be the first sample to demonstrate a quantum criticality, i.e., n = 1.6 down to 20 mK, as shown in Figure 10. Third, the magnetic field or doping dependent coefficient (A_2), representing the cross section of electron-electron scattering and proportional to the quadratic effective electron mass, diverges as approaching the critical magnetic field or critical doping. This means a transition from Fermi liquid to non-Fermi liquid at zero temperature limit. So, there are at least two QCPs that have been revealed, i.e., x_{FS} and x_c. Yet the x_{FS} is linked to the Fermi surface reconstruction, the origin of the second one is still unclear. By measuring the Nernst effect in PCCO from x = 0.13 to 0.17, Tafti proposed that the AF fluctuations cause d-wave pairing, while the AF order competes with superconductivity. The first effect promotes T_c but the second suppresses T_c, therefore the superconductivity dome is shaped by two QCPs [27,87].

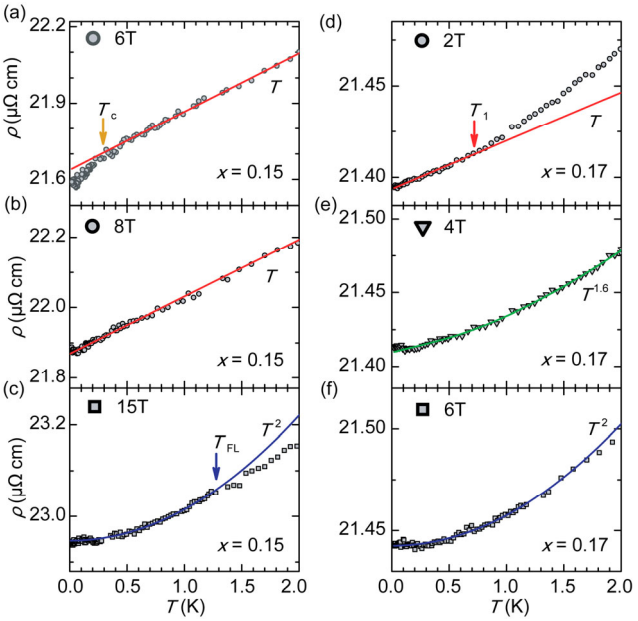

Figure 10 (Color online) The evolution of electrical resistivity $\rho(T)$ for two characteristic superconducting films of LCCO with x = 0.15 (a)–(c) and 0.17 (d)–(f) with applied magnetic fields [27].

5 Order-parameter symmetry

The $d_{x^2-y^2}$ symmetry of hole-doped cuprates has reached consensus, whereas the order-parameter symmetry of electron-doped cuprates is still contentious [9].

Phenomena such as a small shift of leading edge midpoints near the (π, 0) position in ARPES [88] and half-flux quantum observed in tri-crystal junction experiments [89] support a d-wave pairing in optimally doped NCCO. Biswas et al. suggested a transition from d-wave to *s*-wave near optimal doping in PCCO [90]. Magnetic penetration depth measurements showed a similar transition in symmetry [91]. These results may be related to the QCP near the optimal doping [90]. Theoretically, Vojta et al. [92] suggested that *d*-wave symmetry was predominant in the underdoped region, while, $d + id_{xy}$ or $d + is$ became more stable near optimal doping. Accordingly, an illustration of order-parameter symmetry is concluded in Figure 11.

So far, the tunneling experiments are most widely used to probe the information on order-parameter symmetry. For this kind of experiments, zero bias conductance peak (ZBCP) is a typical feature of a superconductor in *d*-wave symmetry [93], stemming from the Andreev reflection between positive and negative phases in a *k*-dependent node gap [94]. For example, ZBCP has been observed in bi-crystal junction of LCCO [95,96]. While, it is not observed in NCCO [97,98] and PLCCO [99].

The absence of ZBCP may indicate a nodeless gap. However, it is important to point out that ZBCP may disappear in certain condition for a *d*-wave symmetry superconductor in tunneling experiments: (1) ZBCP may be suppressed by an increase of disorder in the material [100]; (2) if thermal smearing of the tunneling spectrum is comparable to the width of ZBCP, the latter will be concealed [90,97]; (3) the strong paramagnetism of Nd^{3+} ion may veil the *d*-wave symmetry in NCCO [101]; (4) the coexistence of antiferromagnetism and superconductivity may also bring a puzzle [102].

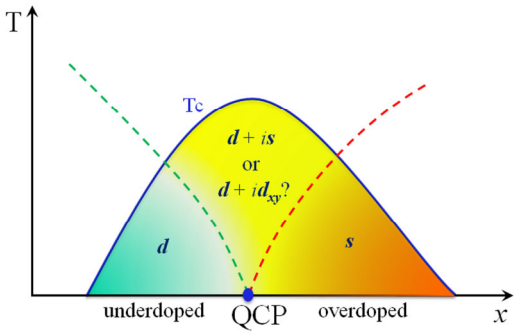

Figure 11 (Color online) The scheme of the symmetry as a function of doping. *x*- and *y*- axes stand for doping and temperature, respectively. The different colors in the superconducting dome represent *d*-wave (green), $d + id_{xy}$ or $d + is$ (yellow), and *s*-wave (red). The QCP associated with the Fermi surface reconstruction is also presented (blue circle) [90–92].

Recently, Dagan et al. [103] carried out point-contact spectra measurements on PCCO from x = 0.13 to 0.19. They found that a modified BTK with a nonmonotonic *d*-wave symmetry could fit the tunneling spectra very well, yet the ZBCP was absent. The nonmonotonic *d*-wave symmetry, with a maximum gap at the hotspots instead of the antinodal points, was firstly revealed by Blumberg et al. [104] in NCCO from a low energy polarized Raman scattering experiment.

However, most of the tunneling measurements were carried out on optimally doped n-type cuprates [43,97,98,105]. The answers to whether the order-parameter symmetry is nonmonotonic *d*-wave or not, and whether it is dependent on doping or not, are still open to deliberation. It is still worthy of performing careful doping dependent tunneling measurements on different electron-doped cuprate systems to clarify these questions.

6 Superconductivity emergent in parent compounds

Recently, the long-standing phase diagram for copper-oxide superconductors has been challenged in the electron-doped side, i.e. the insulating parent compounds have been made superconducting [106,107].

As early as in 1994, Brinkmann et al. [108,109], treated the as-grown PCCO crystal in a higher annealing temperature as well as a longer annealing time. Unexpectedly, the superconducting dome is apparently extended towards the

low Ce doping side. In 2008, Matsumoto et al. reported a two-step annealing process in synthesizing the parent compounds T'-R_2CuO_4(R=Pr, Nd, Sm, Eu and Gd) thin films. Surprisingly, they observed superconductivity in these parent compounds [110]. Krockenberger et al. [106] summarized the new phase diagram as shown in Figure 12.

The distinction between the new synthesis method and the traditional one lies in the post-annealing step. Though the micro-mechanism of the post-annealing step is still open to debate, it is believed that the fine control of oxygen atoms is essential to the appearance of superconductivity [106].

Jin et al. [111] has grown multilayers of electron-doped cuprates, composed of underdoped (or undoped) and overdoped LCCO and PCCO thin films. They found an enhanced or emergent T_c, which is comparable to the T_c of optimally doped LCCO or PCCO. The oxygen diffusion was considered to be the most plausible origin of the T_c enhancement.

Using high-pressure diamond-anvil cell, Rotundu et al found the superconducting T' phase of optimally doped PCCO single crystal (x=0.15) could be partially tuned into insulating T phase, at 2.72 GPa, but the superconductivity of the overdoped sample retained under a pressure up to 32 GPa [67]. These new phenomena stimulate the recognition of the electron-doped cuprates.

7 New developments towards applications

As to electron-doped cuprates, the oxygen reduction annealing process hinders the integration with other functional oxides, such as colossal magnetoresistance and ferroelectrics, of which the better characteristics should be achieved in an oxygenated process. Therefore, some basic electric device configurations, e.g. p-n junctions, cannot be easily realized.

Hoek et al. [112] grew NCCO films by pulsed laser deposition using a non-stoichiometric target with extra copper. After the initial vacuum annealing, an oxygenation annealing process was followed in O_2 pressure of 1 bar. This method enables the integration of electron-doped cuprates with their hole-doped counterparts on single chip. A *p-I-n* junction was then successfully fabricated with an insulating layer sandwiched between the hole- and electron-doped oxides. Remarkable rectifying effect can be achieved with appropriate barrier in such device as shown in Figure 13 [113].

A ramp-edge Josephson junction has been prepared with a heavily underdoped PCCO layer sandwiched between two optimally (over) doped PCCO layers [114,115]. With a special configuration of step junction [116], intrinsic Josephson effect was observed for the first time in PLCCO films [117]. All these efforts are gradually pushing the electron-doped cuprates into practical applications in electronics.

8 Conclusion and perspective

The understanding of the nature of the electron-doped cuprates goes ahead steadily with some important issues remaining unsolved, such as the boundary of the AF order, the origin of the two bands and the QCP at the end of the superconducting dome, the order-parameter sysmmtery, the micro mechanism of the post annealing, etc. Meanwhile, samples of high quality appear more and more crucial for exploring the intrinsic properties, also for the potential applicaions of electronics.

Recently, the newly developing techniques, e.g. electric double layer transistor (EDLT) [118] and combinatorial film deposition [119–124], are being applied to the superconductivity field. The fancy EDLT can generate very large electric field and accumulate high-density charge carriers, succeeding in tuning the superconductivity or electronic states [73,74,125]. The combinatorial techniques can produce films with chemical composition gradiently

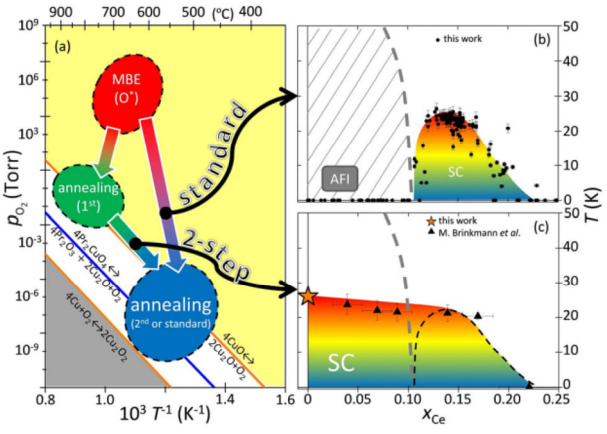

Figure 12 (Color online) Annealing paths of Pr_2CuO_4 and the corresponding electronic phase diagrams [106].

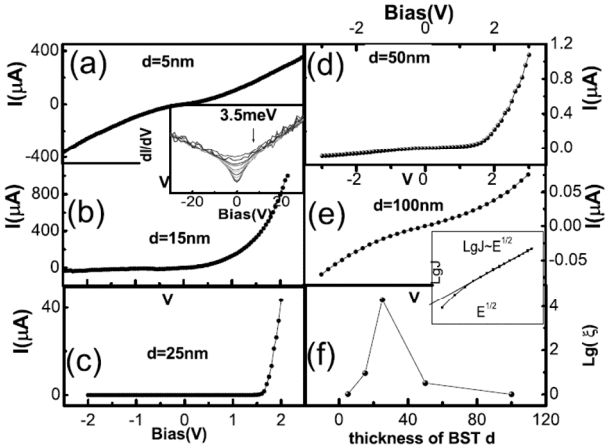

Figure 13 *I-V* curves of the junctions with various thicknesses of BST at 5 K. The largest rectification (>10^4) is obtained for BST of ~25 nm [113].

distributed. Both the techniques are powerful in modulating the samples. An attempt to employ these advanced techniques will supply a chance to build a more precise phase diagram and shed light on the comprehension of electron-doped cuprates.

This work was supported by the Strategic Priority Research Program (B) of the Chinese Academy of Sciences (Grant No. XDB07020100), the National Natural Science Foundation of China (Grant No. 11474338), and the National Key Basic Research Program of China (Grant No. 2015CB921000).

1 Bednorz J G, Müller K A. Possible high T_c superconductivity in the Ba-La-Cu-O system. Z Phys B: Condens Matter, 1986, 64: 189–193
2 Schilling A, Cantoni M, Guo J D, et al. Superconductivity above 130 K in the Hg-Ba-Ca-Cu-O system. Nature, 1993, 363: 56–58
3 Gao L, Xue Y Y, Chen F, et al. Superconductivity up to 164 K in $HgBa_2Ca_{m-1}Cu_mO_{2m+2+\delta}$($m$ =1, 2, and 3) under quasihydrostatic pressures. Phys Rev B, 1994, 50: 4260–4263
4 Tokura Y, Takagi H, Uchida S. A superconducting copper oxide compound with electrons as the charge carriers. Nature, 1989, 337: 345–347
5 Ayoub N Y, Markert J T, Early E A, et al. A comparative compositional study of $Ln_{2-x}M_xCuO_{4-y}$ electron-doped superconductors. Phys C, 1990, 165: 469–474
6 Beille J, Gerber A, Grenet T, et al. Superconducting properties of $Ln_{2-x}M_xCuO_{4-y}$ (Ln = Pr, Nd, Sm, Eu, M = Ce, Th) under pressure up to 100-kbar. J Less-Common Met, 1990, 164: 800–807
7 Dalichaouch Y, Lee B W, Seaman C L, et al. Upper critical-field of a $Sm_{1.85}Ce_{0.15}CuO_{4-y}$ single-crystal-interaction between superconductivity and antiferromagnetic order in copper oxides. Phys Rev Lett, 1990, 64: 599–602
8 Dalichaouch Y, Deandrade M C, Maple M B. Synthesis, transport, and magnetic-properties of $Ln_{2-x}Ce_xCuO_{4-y}$ single-crystals (Ln = Nd, Pr, Sm). Phys C, 1993, 218: 309–315
9 Armitage N P, Fournier P, Greene R L. Progress and perspectives on electron-doped cuprates. Rev Mod Phys, 2010, 82: 2421–2487
10 Witt T J. Accurate determination of 2e/h in Y-Ba-Cu-O josephson junctions. Phys Rev Lett, 1988, 61: 1423–1426
11 Vanbentum P J M, Hoevers H F C, Vankempen H, et al. Determination of the energy-gap in $YBa_2Cu_3O_{7-\delta}$ by tunneling, far infrared reflection and Andreev reflection. Phys C, 1988, 153: 1718–1723
12 Gough C E, Colclough M S, Forgan E M, et al. Flux-quantization in a high-T_c superconductor. Nature, 1987, 326: 855–855
13 Gammel P L, Polakos P A, Rice C E, et al. Little-parks oscillations of T_c in patterned microstructures of the oxide superconductor $YBa_2Cu_3O_7$-experimental limits on fractional-statistics-particle theories. Phys Rev B, 1990, 41: 2593–2596
14 Campuzano J C, Ding H, Norman M R, et al. Direct observation of particle-hole mixing in the superconducting state by angle-resolved photoemission. Phys Rev B, 1996, 53: 14737–14740
15 Takigawa M, Hammel P C, Heffner R H, et al. Spin susceptibility in superconducting $YBa_2Cu_3O_7$ from Cu-63 knight-shift. Phys Rev B, 1989, 39: 7371–7374
16 Hardy W N, Bonn D A, Morgan D C, et al. Precision-measurements of the temperature-dependence of lambda in $YBa_2Cu_3O_{6.95}$: Strong evidence for nodes in the gap function. Phys Rev Lett, 1993, 70: 3999–4002
17 Damascelli A, Hussain Z, Shen Z X. Angle-resolved photoemission studies of the cuprate superconductors. Rev Mod Phys, 2003, 75: 473–541
18 Tsuei C C, Kirtley J R. Pairing symmetry in cuprate superconductors. Rev Mod Phys, 2000, 72: 969–1016
19 Wright D A, Emerson J P, Woodfield B F, et al. Low-temperature specific heat of $YBa_2Cu_3O_{7-\delta}$, $0\leqslant\delta\leqslant0.2$: Evidence for d-Wave pairing. Phys Rev Lett, 1999, 82: 1550–1553
20 Sutherland M, Hawthorn D G, Hill R W, et al. Thermal conductivity across the phase diagram of cuprates: Low-energy quasiparticles and doping dependence of the superconducting gap. Phys Rev B, 2003, 67: 174520
21 Paglione J, Greene R L. High-temperature superconductivity in iron-based materials. Nat Phys, 2010, 6: 645–658
22 Scalapino D J. A common thread: The pairing interaction for unconventional superconductors. Rev Mod Phys, 2012, 84: 1383–1417; Li S, Yang H, Fang D L, et al. Strong coupling superconductivity and prominent superconducting fluctuations in the new superconductor $Bi_4O_4S_3$. Sci China-Phys Mech Astron, 2013, 56: 2019–2025; Chen R Y, Dong T, Wang H P, et al. Ultrafast quasiparticle dynamics in spin-density-wave LaOFeAs single crystal. Sci China-Phys Mech Astron, 2013, 56: 2395–2398
23 Norman M R. The Challenge of unconventional superconductivity. Science, 2011, 332: 196–200
24 Norman M R. Chasing arcs in cuprate superconductors. Science, 2009, 325: 1080–1081
25 Cooper R A, Wang Y, Vignolle B, et al. Anomalous criticality in the electrical resistivity of $La_{2-x}Sr_xCuO_4$. Science, 2009, 323: 603–607
26 Jin K, Butch N P, Kirshenbaum K, et al. Link between spin fluctuations and electron pairing in copper oxide superconductors. Nature, 2011, 476: 73–75
27 Butch N P, Jin K, Kirshenbaum K, et al. Quantum critical scaling at the edge of Fermi liquid stability in a cuprate superconductor. P Natl Acad Sci USA, 2012, 109: 8440–8444
28 Tohyama T. Recent progress in physics of high-temperature superconductors. Jpn J Appl Phys, 2012, 51: 010004
29 Moritz B, Johnston S, Devereaux T P, et al. Investigation of particle-hole asymmetry in the cuprates via electronic raman scattering. Phys Rev B, 2011, 84: 235114
30 Ishii K, Fujita M, Sasaki T, et al. High-energy spin and charge excitations in electron-doped copper oxide superconductors. Nat Commun, 2014, 5: 3714
31 Tanatar M A, Ni N, Thaler A, et al. Pseudogap and its critical point in the heavily doped $Ba(Fe_{1-x}Co_x)_2As_2$ from c-axis resistivity measurements. Phys Rev B, 2010, 82: 134528
32 Middey S, Kareev M, Meyers D, et al. Epitaxial stabilization of ultra thin films of electron doped manganites. Appl Phys Lett, 2014, 104: 202409
33 Saadaoui H, Salman Z, Luetkens H, et al. The phase diagram of electron-doped $La_{2-x}Ce_xCuO_{4-\delta}$. Nat Commun, 2015, 6: 6041
34 Marshall D S, Dessau D S, Loeser A G, et al. Unconventional electronic structure evolution with hole doping in $Bi_2Sr_2CaCu_2O_{8+\delta}$: Angle-resolved photoemission results. Phys Rev Lett, 1996, 76: 4841–4844
35 Ding H, Yokoya T, Campuzano J C, et al. Spectroscopic evidence for a pseudogap in the normal state of underdoped high-T_c superconductors. Nature, 1996, 382: 51–54
36 Yu W, Higgins J S, Bach P, et al. Transport evidence of a magnetic quantum phase transition in electron-doped high-temperature superconductors. Phys Rev B, 2007, 76: 020503
37 Dagan Y, Qazilbash M M, Hill C P, et al. Evidence for a quantum phase transition in $Pr_{2-x}Ce_xCuO_{4-\delta}$ from transport measurements. Phys Rev Lett, 2004, 92: 167001
38 Motoyama E M, Yu G, Vishik I M, et al. Spin correlations in the electron-doped high-transition-temperature superconductor $Nd_{2-x}Ce_xCuO_{4\pm\delta}$. Nature, 2007, 445: 186–189
39 Sachdev S. Where is the quantum critical point in the cuprate superconductors? Phys Status Solidi B, 2010, 247: 537–543
40 Biswas A, Fournier P, Smolyaninova V N, et al. Gapped tunneling spectra in the normal state of $Pr_{2-x}Ce_xCuO_4$. Phys Rev B, 2001, 64: 104519
41 Alff L, Krockenberger Y, Welter B, et al. A hidden pseudogap under the "dome" of superconductivity in electron-doped high-temperature superconductors. Nature, 2003, 422: 698–701
42 Dagan Y, Qazilbash M M, Greene R L. Tunneling into the normal

state of $Pr_{2-x}Ce_xCuO_4$. Phys Rev Lett, 2005, 94: 187003
43 Shan L, Wang Y L, Huang Y, et al. Distinction between the normal-state gap and superconducting gap of electron-doped cuprates. Phys Rev B, 2008, 78: 014505
44 Startseva T, Timusk T, Puchkov A V, et al. Temperature evolution of the pseudogap state in the infrared response of underdoped $La_{2-x}Sr_xCuO_4$. Phys Rev B, 1999, 59: 7184–7190
45 Berg E, Fradkin E, Kivelson S A. Charge-4e superconductivity from pair-density-wave order in certain high-temperature superconductors. Nat Phys, 2009, 5: 830–833
46 Lawler M J, Fujita K, Lee J, et al. Intra-unit-cell electronic nematicity of the high-T_c copper-oxide pseudogap states. Nature, 2010, 466: 347–351
47 Fausti D, Tobey R I, Dean N, et al. Light-induced superconductivity in a stripe-ordered cuprate. Science, 2011, 331: 189–191
48 Mesaros A, Fujita K, Eisaki H, et al. Topological defects coupling smectic modulations to intra-unit-cell nematicity in cuprates. Science, 2011, 333: 426–430
49 Daou R, Chang J, LeBoeuf D, et al. Broken rotational symmetry in the pseudogap phase of a high-T_c superconductor. Nature, 2010, 463: 519–522
50 Neto E H D S, Comin R, He F Z, et al. Charge ordering in the electron-doped superconductor $Nd_{2-x}Ce_xCuO_4$. Science, 2015, 347: 283–285
51 Onose Y, Taguchi Y, Ishikawa T, et al. Anomalous pseudogap formation in a nonsuperconducting crystal of $Nd_{1.85}Ce_{0.15}CuO_{4+y}$: Implication of charge ordering. Phys Rev Lett, 1999, 82: 5120–5123
52 Jin K, He G, Zhang X H, et al. Anomalous magnetoresistance in the spinel superconductor $LiTi_2O_4$. Nat Commun, 2015, 6: 7183
53 LeBoeuf D, Doiron-Leyraud N, Levallois J, et al. Electron pockets in the Fermi surface of hole-doped high-T_c superconductors. Nature, 2007, 450: 533–536
54 Doiron-Leyraud N, Proust C, LeBoeuf D, et al. Quantum oscillations and the Fermi surface in an underdoped high-T_c superconductor. Nature, 2007, 447: 565–568
55 Sebastian S E, Harrison N, Balakirev F F, et al. Normal-state nodal electronic structure in underdoped high-T_c copper oxides. Nature, 2014, 511: 61–64
56 Riggs S C, Vafek O, Kemper J B, et al. Heat capacity through the magnetic-field-induced resistive transition in an underdoped high-temperature superconductor. Nat Phys, 2011, 7: 332–335
57 Jiang W, Mao S N, Xi X X, et al. Anomalous transport-properties in superconducting $Nd_{1.85}Ce_{0.15}Cuo_{4\pm\delta}$. Phys Rev Lett, 1994, 73: 1291–1294
58 Armitage N P, Ronning F, Lu D H, et al. Doping dependence of an n-type cuprate superconductor investigated by angle-resolved photoemission spectroscopy. Phys Rev Lett, 2002, 88: 257001
59 Jin K, Zhu B Y, Wu B X, et al. Low-temperature Hall effect in electron-doped superconducting $La_{2-x}Ce_xCuO_4$ thin films. Phys Rev B, 2008, 78: 174521
60 Jin K, Zhu B Y, Yuan J, et al. Evolution of charge carriers for transport in electron-doped cuprate superconductor $La_{1.89}Ce_{0.11}CuO_4$ thin films. Phys Rev B, 2007, 75: 214501
61 Charikova T B, Shelushinina N G, Harus G I, et al. Doping effect on the anomalous behavior of the Hall effect in electron-doped superconductor $Nd_{2-x}Ce_xCuO_{4+\delta}$. Phys C, 2012, 483: 113–118
62 Jin K, Wu B X, Zhu B Y, et al. Sign reversal of the Hall resistance in the mixed-state of $La_{1.89}Ce_{0.11}CuO_4$ and $La_{1.89}Ce_{0.11}(Cu_{0.99}Co_{0.01})O_4$ thin films. Phys C, 2012, 479: 53–56
63 Lin J, Millis A J. Theory of low-temperature Hall effect in electron-doped cuprates. Phys Rev B, 2005, 72: 214506
64 Xiang T, Luo H G, Lu D H, et al. Intrinsic electron and hole bands in electron-doped cuprate superconductors. Phys Rev B, 2009, 79: 014524
65 Jiang W, Mao S, Xi X, et al. Anomalous transport properties in superconducting $Nd_{1.85}Ce_{0.15}CuO_{4\pm\delta}$. Phys Rev Lett, 1994, 73: 1291– 1294
66 Horio M, Adachi T, Mori Y, et al. Suppression of the antiferromagnetic pseudogap in the electron-doped high-temperature superconductor by "protect annealing". arXiv:1502.03395
67 Rotundu C R, Struzhkin V V, Somayazulu M S, et al. High-pressure effects on single crystals of electron-doped $Pr_{2-x}Ce_xCuO_4$. Phys Rev B, 2013, 87: 024506
68 Segawa K, Ando Y. Doping n-type carriers by La substitution for Ba in the $YBa_2Cu_3O_y$ system. Phys Rev B, 2006, 74: 100508
69 Zeng S W, Wang X, Lu W M, et al. Metallic state in La-doped $YBa_2Cu_3O_y$ thin films with n-type charge carriers. Phys Rev B, 2012, 86: 045124
70 Segawa K, Kofu M, Lee S H, et al. Zero-doping state and electron-hole asymmetry in an ambipolar cuprate. Nat Phys, 2010, 6: 579–583
71 Sachdev S. Quantum criticality: Competing ground states in low dimensions. Science, 2000, 288: 475–480
72 von Lohneysen H, Rosch A, Vojta M, et al. Fermi-liquid instabilities at magnetic quantum phase transitions. Rev Mod Phys, 2007, 79: 1015–1075; Jin C Q, Wang X C, Liu Q Q, et al. New quantum matters: Build up versus high pressure tuning. Sci China-Phys Mech Astron, 2013, 56: 2337–2350
73 Leng X, Garcia-Barriocanal J, Bose S, et al. Electrostatic control of the evolution from a superconducting phase to an insulating phase in ultrathin $YBa_2CaCu_3O_{7-x}$ films. Phys Rev Lett, 2011, 107: 027001
74 Bollinger A T, Dubuis G, Yoon J, et al. Superconductor-insulator transition in $La_{2-x}Sr_xCuO_4$ at the pair quantum resistance. Nature, 2011, 472: 458–460
75 Daou R, Doiron-Leyraud N, LeBoeuf D, et al. Linear temperature dependence of resistivity and change in the Fermi surface at the pseudogap critical point of a high-T_c superconductor. Nat Phys, 2009, 5: 31–34
76 Fournier P, Mohanty P, Maiser E, et al. Insulator-metal crossover near optimal doping in $Pr_{2-x}Ce_xCuO_4$: Anomalous normal-state low temperature resistivity. Phys Rev Lett, 1998, 81: 4720–4723
77 Moriya T, Ueda K. Spin fluctuations and high temperature superconductivity. Adv Phys, 2000, 49: 555–606
78 Rosch A. Magnetotransport in nearly antiferromagnetic metals. Phys Rev B, 2000, 62: 4945–4962
79 Doiron-Leyraud N, Auban-Senzier P, de Cotret S R, et al. Correlation between linear resistivity and T_c in the Bechgaard salts and the pnictide superconductor $Ba(Fe_{1-x}Co_x)_2As_2$. Phys Rev B, 2009, 80: 214531
80 Bourbonnais C, Sedeki A. Link between antiferromagnetism and superconductivity probed by nuclear spin relaxation in organic conductors. Phys Rev B, 2009, 80: 085105
81 Taillefer L. Scattering and pairing in cuprate superconductors. Annu Rev Condens Matter Phys, 2010, 1: 51–70
82 Jin K, Yuan J, Zhao L, et al. Coexistence of superconductivity and ferromagnetism in a dilute cobalt-doped $La_{1.89}Ce_{0.11}CuO_{4\pm\delta}$ system. Phys Rev B, 2006, 74: 094518
83 Jin K, Zhang X H, Bach P, et al. Evidence for antiferromagnetic order in $La_{2-x}Ce_xCuO_4$ from angular magnetoresistance measurements. Phys Rev B, 2009, 80: 012501
84 Fujita M, Matsuda M, Lee S H, et al. Low-energy spin fluctuations in the ground states of electron-doped $Pr_{1-x}LaCe_xCuO_{4+\delta}$ cuprate superconductors. Phys Rev Lett, 2008, 101: 107003
85 Sedeki A, Bergeron D, Bourbonnais C. Extended quantum criticality of low-dimensional superconductors near a spin-density-wave instability. Phys Rev B, 2012, 85: 165129
86 Jin K, Zhu B Y, Wu B X, et al. Normal-state transport in electron-doped $La_{2-x}Ce_xCuO_4$ thin films in magnetic fields up to 40 Tesla. Phys Rev B, 2008, 77: 172503
87 Tafti F F, Laliberte F, Dion M, et al. Nernst effect in the electron-doped cuprate superconductor $Pr_{2-x}Ce_xCuO_4$: Superconducting fluctuations, upper critical field $H_{c2,}$ and the origin of the T_c dome. Phys Rev B, 2014, 90: 024519
88 Armitage N P, Lu D H, Feng D L, et al. Superconducting gap anisotropy in $Nd_{1.85}Ce_{0.15}CuO_4$: Results from photoemission. Phys Rev Lett, 2001, 86: 1126–1129
89 Tsuei C C, Kirtley J R. Phase-sensitive evidence for *d*-wave pairing symmetry in electron-doped cuprate superconductors. Phys Rev Lett,

2000, 85: 182–185
90 Biswas A, Fournier P, Qazilbash M M, et al. Evidence of a *d*- to *s*-wave pairing symmetry transition in the electron-doped cuprate superconductor $Pr_{2-x}Ce_xCuO_4$. Phys Rev Lett, 2002, 88: 207004
91 Skinta J A, Kim M S, Lemberger T R, et al. Evidence for a transition in the pairing symmetry of the electron-doped cuprates $La_{2-x}Ce_xCuO_{4-y}$ and $Pr_{2-x}Ce_xCuO_{4-y}$. Phys Rev Lett, 2002, 88: 207005
92 Vojta M, Zhang Y, Sachdev S. Quantum phase transitions in *d*-wave superconductors. Phys Rev Lett, 2000, 85: 4940–4943
93 Deutscher G. Andreev-saint-james reflections: A probe of cuprate superconductors. Rev Mod Phys, 2005, 77: 109–135
94 Tanaka Y, Kashiwaya S. Theory of tunneling spectroscopy of *d*-wave superconductors. Phys Rev Lett, 1995, 74: 3451–3454
95 Chesca B, Seifried M, Dahm T, et al. Observation of Andreev bound states in bicrystal grain-boundary Josephson junctions of the electron-doped superconductor $La_{2-x}Ce_xCuO_{4-y}$. Phys Rev B, 2005, 71: 104504
96 Wagenknecht M, Koelle D, Kleiner R, et al. Phase diagram of the electron-doped $La_{2-x}Ce_xCuO_4$ cuprate superconductor from Andreev bound states at grain boundary junctions. Phys Rev Lett, 2008, 100: 227001
97 Kashiwaya S, Ito T, Oka K, et al. Tunneling spectroscopy of superconducting $Nd_{1.85}Ce_{0.15}CuO_{4-\delta}$. Phys Rev B, 1998, 57: 8680–8686
98 Shan L, Huang Y, Gao H, et al. Distinct pairing symmetries in $Nd_{1.85}Ce_{0.15}CuO_{4-y}$ and $La_{1.89}Sr_{0.11}CuO_4$ single crystals: Evidence from comparative tunneling measurements. Phys Rev B, 2005, 72: 144506
99 Shan L, Huang Y, Wang Y L, et al. Weak-coupling Bardeen-Cooper-Schrieffer superconductivity in the electron-doped cuprate superconductors. Phys Rev B, 2008, 77: 014526
100 Aprili M, Covington M, Paraoanu E, et al. Tunneling spectroscopy of the quasiparticle Andreev bound state in ion-irradiated $YBa_2Cu_3O_{7-\delta}$/Pb junctions. Phys Rev B, 1998, 57: R8139–R8142
101 Alff L, Meyer S, Kleefisch S, et al. Anomalous low temperature behavior of superconducting $Nd_{1.85}Ce_{0.15}CuO_{4-y}$. Phys Rev Lett, 1999, 83: 2644–2647
102 Liu C S, Wu W C. Theory of point-contact spectroscopy in electron-doped cuprate superconductors. Phys Rev B, 2007, 76: 220504
103 Dagan Y, Beck R, Greene R L. Dirty superconductivity in the electron-doped cuprate $Pr_{2-x}Ce_xCuO_{4-\delta}$: Tunneling study. Phys Rev Lett, 2007, 99: 147004
104 Blumberg G, Koitzsch A, Gozar A, et al. Nonmonotonic d_{x2-y2} superconducting order parameter in $Nd_{2-x}Ce_xCuO_4$. Phys Rev Lett, 2002, 88: 107002
105 Mourachkine A. Andreev reflections and tunneling spectroscopy on underdoped $Nd_{1.85}Ce_{0.15}CuO_{4-\delta}$. Europhys Lett, 2000, 50: 663–667
106 Krockenberger Y, Irie H, Matsumoto O, et al. Emerging superconductivity hidden beneath charge-transfer insulators. Sci Rep, 2013, 3: 2235
107 Krockenberger Y, Eleazer B, Irie H, et al. Superconducting- and insulating-ground states in La_2CuO_4 structural isomers. J Phys Soc Jpn, 2014, 83: 114602
108 Brinkmann M, Rex T, Bach H, et al. Extended superconducting concentration range observed in $Pr_{2-x}Ce_xCuO_{4-\delta}$. Phys Rev Lett, 1995, 74: 4927–4930
109 Brinkmann M, Bach H, Westerholt K. Electrical resistivity study of metallic $Pr_{2-x}Ce_xCuO_{4+\delta}$ single crystals over a broad concentration and temperature range. Phys C, 1997, 292: 104–116
110 Matsumoto O, Utsuki A, Tsukada A, et al. Superconductivity in undoped *T'*-RE_2CuO_4 with T_c over 30 K. Phys C, 2008, 468: 1148–1151
111 Jin K, Bach P, Zhang X H, et al. Anomalous enhancement of the superconducting transition temperature of electron-doped $La_{2-x}Ce_xCuO_4$ and $Pr_{2-x}Ce_xCuO_4$ cuprate heterostructures. Phys Rev B, 2011, 83: 060511
112 Hoek M, Coneri F, Leusink D P, et al. Effect of high oxygen pressure annealing on superconducting $Nd_{1.85}Ce_{0.15}CuO_4$ thin films by pulsed laser deposition from Cu-enriched targets. Supercond Sci Technol, 2014, 27: 044017
113 Yuan J, Wu H, Cao L X, et al. Metallic oxide *p-I-n* junctions with ferroelectric as the barrier. Appl Phys Lett, 2007, 90: 102113
114 Roberge G, Charpentier S, Godin-Proulx S, et al. Ramp-edge Josephson junctions made of $Pr_{2-x}Ce_xCuO_{4\pm\delta}$ electrodes and barriers. J Appl Phys, 2011, 109: 073912
115 Charpentier S, Roberge G, Godin-Proulx S, et al. Proximity effect in electron-doped cuprate Josephson junctions. Appl Phys Lett, 2011, 99: 032511
116 Wang H B, Chen J, Tachiki T, et al. Intrinsic Josephson junctions in oxygen-deficient $YBa_2Cu_3O_{7-\delta}$ film deposited on a substrate step. J Appl Phys, 1999, 85: 3740–3744
117 Yuan J, Wang H B, Iguchi I, et al. Growth of electron-doped superconductor $Pr_{0.9}LaCe_{0.1}CuO_4$ films and their applications to intrinsic Josephson iunctions. IEEE Trans Appl Supercond, 2009, 19: 3443–3446
118 Hwang H Y, Iwasa Y, Kawasaki M, et al. Emergent phenomena at oxide interfaces. Nat Mater, 2012, 11: 103–113
119 Briceno G, Chang H Y, Sun X D, et al. A class of cobalt oxide magnetoresistance materials discovered with combinatorial synthesis. Science, 1995, 270: 273–275
120 Danielson E, Devenney M, Giaquinta D M, et al. A rare-earth phosphor containing one-dimensional chains identified through combinatorial methods. Science, 1998, 279: 837–839
121 Matsumoto Y, Murakami M, Shono T, et al. Room-temperature ferromagnetism in transparent transition metal-doped titanium dioxide. Science, 2001, 291: 854–856
122 Wang J S, Yoo Y, Gao C, et al. Identification of a blue photoluminescent composite material from a combinatorial library. Science, 1998, 279: 1712–1714
123 Xiang X D, Sun X D, Briceno G, et al. A combinatorial approach to materials discovery. Science, 1995, 268: 1738–1740
124 Jin K, Suchoski R, Fackler S, et al. Combinatorial search of superconductivity in Fe-B composition spreads. APL Mater, 2013, 1: 042101
125 Carmeli I, Lewin A, Flekser E, et al. Tuning the critical temperature of cuprate superconductor films with self-assembled organic layers. Angew Chem-Int Edit, 2012, 51: 7162–7165